Supplement of Atmos. Chem. Phys., 20, 6991–7019, 2020
https://doi.org/10.5194/acp-20-6991-2020-supplement

Atmospheric Chemistry and Physics
Open Access
EGU

Supplement of

Quantifying uncertainties of climate signals in chemistry climate models related to the 11-year solar cycle – Part 1: Annual mean response in heating rates, temperature, and ozone

Markus Kunze et al.

Correspondence to: Markus Kunze (markus.kunze@met.fu-berlin.de)

Table S1: Solar cycle spectral solar irradiance (SSI) variations for Solar Cycles indicated in the first row relative to ATLAS3 (ΔSSI) in % and relative contribution of SSI changes to the TSI change ($\frac{\Delta SSI}{\Delta TSI}$) in % for the Lyman-$\alpha$ (121.5 nm), Far-UV (121–200 nm), Herzberg continuum/Hartley bands (201–242 nm), Hartley-/Huggings-bands (243–380 nm) and visible (381–780 nm) spectral ranges.

Time period	SSI dataset	121.5 nm		121–200 nm		201–242 nm		243–380 nm		381–780 nm	
		ΔSSI	$\frac{\Delta SSI}{\Delta TSI}$	ΔSSI	$\frac{\Delta SSI}{\Delta TSI}$	ΔSSI	$\frac{\Delta SSI}{\Delta TSI}$	ΔSSI	$\frac{\Delta SSI}{\Delta TSI}$	ΔSSI	$\frac{\Delta SSI}{\Delta TSI}$
Cycle 21 descent Max:Dec.1979 Min:Sep.1986	NRLSSI1	45.602	0.214	11.373	0.913	3.599	4.300	0.311	20.748	0.109	55.521
	NRLSSI2	51.609	0.228	11.668	0.882	3.360	3.778	0.402	25.251	0.095	45.247
	SATIRE-T	47.283	0.199	10.081	0.724	3.445	3.684	0.592	35.363	0.106	48.028
	SATIRE-S	47.178	0.281	9.907	1.008	2.987	4.523	0.477	40.368	0.069	44.130
	CMIP6	49.405	0.250	10.788	0.932	3.175	4.080	0.440	31.585	0.082	44.785
Cycle 22 ascent Max:Nov.1989 Min:Sep.1986	NRLSSI1	50.740	0.250	12.673	1.067	3.994	5.006	0.319	22.315	0.104	55.470
	NRLSSI2	56.657	0.273	12.808	1.053	3.668	4.488	0.407	27.845	0.081	42.196
	SATIRE-T	44.322	0.247	9.454	0.899	3.235	4.580	0.529	41.801	0.075	45.107
	SATIRE-S	59.989	0.331	12.634	1.191	3.756	5.269	0.576	45.149	0.070	41.540
	CMIP6	58.338	0.300	12.722	1.117	3.715	4.855	0.492	35.938	0.076	42.139
Cycle 22 descent-2 Max:Nov.1989 Min:Nov.1994	NRLSSI1	44.286	0.266	11.067	1.137	3.482	5.324	0.268	22.913	0.084	54.902
	NRLSSI2	50.377	0.291	11.388	1.125	3.257	4.788	0.354	29.039	0.066	41.415
	SATIRE-T	35.572	0.297	7.576	1.081	2.583	5.486	0.407	48.288	0.047	42.340
	SATIRE-S	57.481	0.329	12.090	1.183	3.601	5.244	0.552	44.874	0.068	42.130
	CMIP6	53.943	0.309	11.741	1.149	3.431	4.997	0.453	36.855	0.068	41.856
Cycle 22 descent Max:Nov.1989 Min:Jun.1996	NRLSSI1	49.420	0.250	12.343	1.066	3.890	4.999	0.311	22.306	0.102	55.503
	NRLSSI2	53.857	0.279	12.175	1.078	3.485	4.594	0.384	28.299	0.075	42.076
	SATIRE-T	46.024	0.233	9.820	0.848	3.363	4.321	0.557	39.972	0.085	46.134
	SATIRE-S	64.121	0.304	13.546	1.096	4.044	4.869	0.629	42.293	0.085	43.436
	CMIP6	59.005	0.291	12.862	1.083	3.767	4.722	0.507	35.494	0.080	42.850
Cycle 23 ascent Max:Mar.2000 Min:Jun.1996	NRLSSI1	40.457	0.286	10.116	1.223	3.177	5.716	0.237	23.772	0.070	53.692
	NRLSSI2	42.445	0.360	9.594	1.388	2.730	5.879	0.274	32.971	0.040	36.438
	SATIRE-T	27.988	0.383	5.989	1.399	2.066	7.180	0.312	60.660	0.025	37.320
	SATIRE-S	49.546	0.473	10.446	1.704	3.041	7.380	0.439	59.580	0.034	35.442
	CMIP6	46.007	0.407	10.021	1.514	2.887	6.492	0.357	44.849	0.037	35.713

Table S2: Solar cycle SSI variations for the average of the five Solar Cycle amplitudes of Table S1 relative to ATLAS3 (ΔSSI) in % and relative contribution of SSI changes to the TSI change ($\frac{\Delta SSI}{\Delta TSI}$) in % for the Lyman-$\alpha$ (121.5 nm), Far-UV (121–200 nm), Herzberg continuum/Hartley bands (201–242 nm), Hartley-/Huggings-bands (243–380 nm) and visible (381–780 nm) spectral ranges. $\pm$ 95% CI indicates the confidence interval.

Time period	SSI dataset	121.5 nm		121–200 nm		201–242 nm		243–380 nm		381–780 nm	
		ΔSSI	$\frac{\Delta SSI}{\Delta TSI}$	ΔSSI	$\frac{\Delta SSI}{\Delta TSI}$	ΔSSI	$\frac{\Delta SSI}{\Delta TSI}$	ΔSSI	$\frac{\Delta SSI}{\Delta TSI}$	ΔSSI	$\frac{\Delta SSI}{\Delta TSI}$
Average Cycle	NRLSSI1	46.101	0.253	11.514	1.081	3.628	5.069	0.289	22.411	0.094	55.018
	$\pm$ 95% CI	4.576	0.029	1.138	0.127	0.363	0.578	0.039	1.228	0.018	0.871
	NRLSSI2	50.989	0.286	11.527	1.105	3.300	4.705	0.364	28.681	0.071	41.474
	$\pm$ 95% CI	5.931	0.053	1.341	0.203	0.393	0.843	0.061	3.098	0.023	3.533
	SATIRE-T	40.238	0.272	8.584	0.990	2.938	5.050	0.479	45.217	0.067	43.786
	$\pm$ 95% CI	9.150	0.079	1.945	0.291	0.660	1.504	0.129	10.883	0.035	4.617
	SATIRE-S	55.663	0.344	11.725	1.236	3.486	5.457	0.535	46.453	0.065	41.335
	$\pm$ 95% CI	7.910	0.084	1.685	0.302	0.510	1.241	0.085	8.435	0.021	3.832
	CMIP6	53.340	0.311	11.627	1.159	3.395	5.029	0.450	36.944	0.069	41.468
	$\pm$ 95% CI	6.249	0.065	1.362	0.239	0.411	0.988	0.065	5.392	0.020	3.792

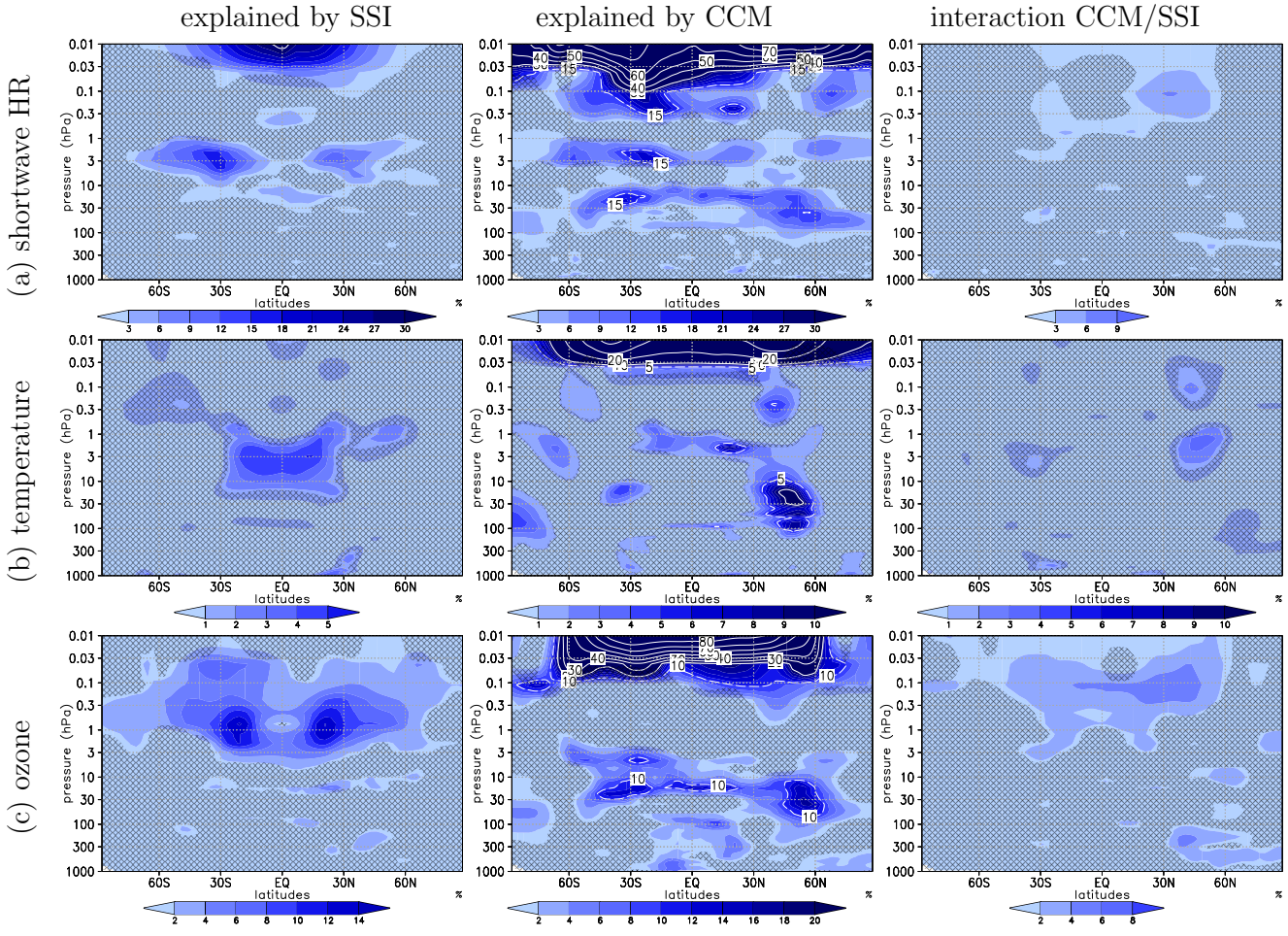

Figure S1: As Figure 4 in the main text, but without the simulations using the SATIRE-T SSI data set. Left column: Percentage of signal variance (square of white contours of left figures) explained by systematic differences between forcing SSI data sets ($R_{a,B}$ Equation A11, blue shading). The white contours indicate levels of explained variance larger than the range of shading. Middle column: as left column but for systematic differences between CCMs ($R_{a,A}$ Equation A11). Right column: as left column but for signal variance explained by the interaction of the CCM and the SSI data set treatments ($R_{a,AB}$ Equation A12). The grey hatching masks areas where the ratio of explained variance does not pass a test for statistical significance ($p > 5$ %).

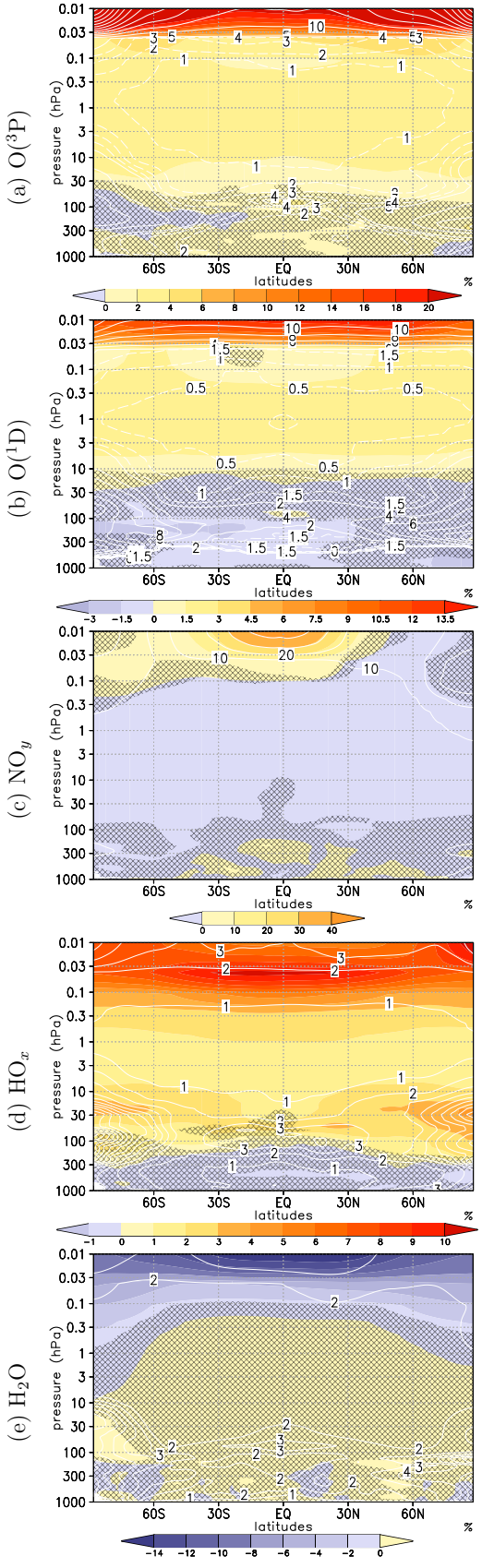

Figure S2: Annual mean 11–year solar cycle response (shaded) and signal variance (white contours) in terms of the solar response annual standard deviation for (a) $O(^3P)$, (b) $O(^1D)$, (c) NO_y, (d) HO_x, and (e) H_2O mixing ratios. Solar signal derived as ensemble mean over both models and all SSI data sets; solar minimum SSI based on ATLAS3 reference state. The grey hatching masks areas where the solar cycle response does not pass a test for statistical significance ($p > 5$ %).

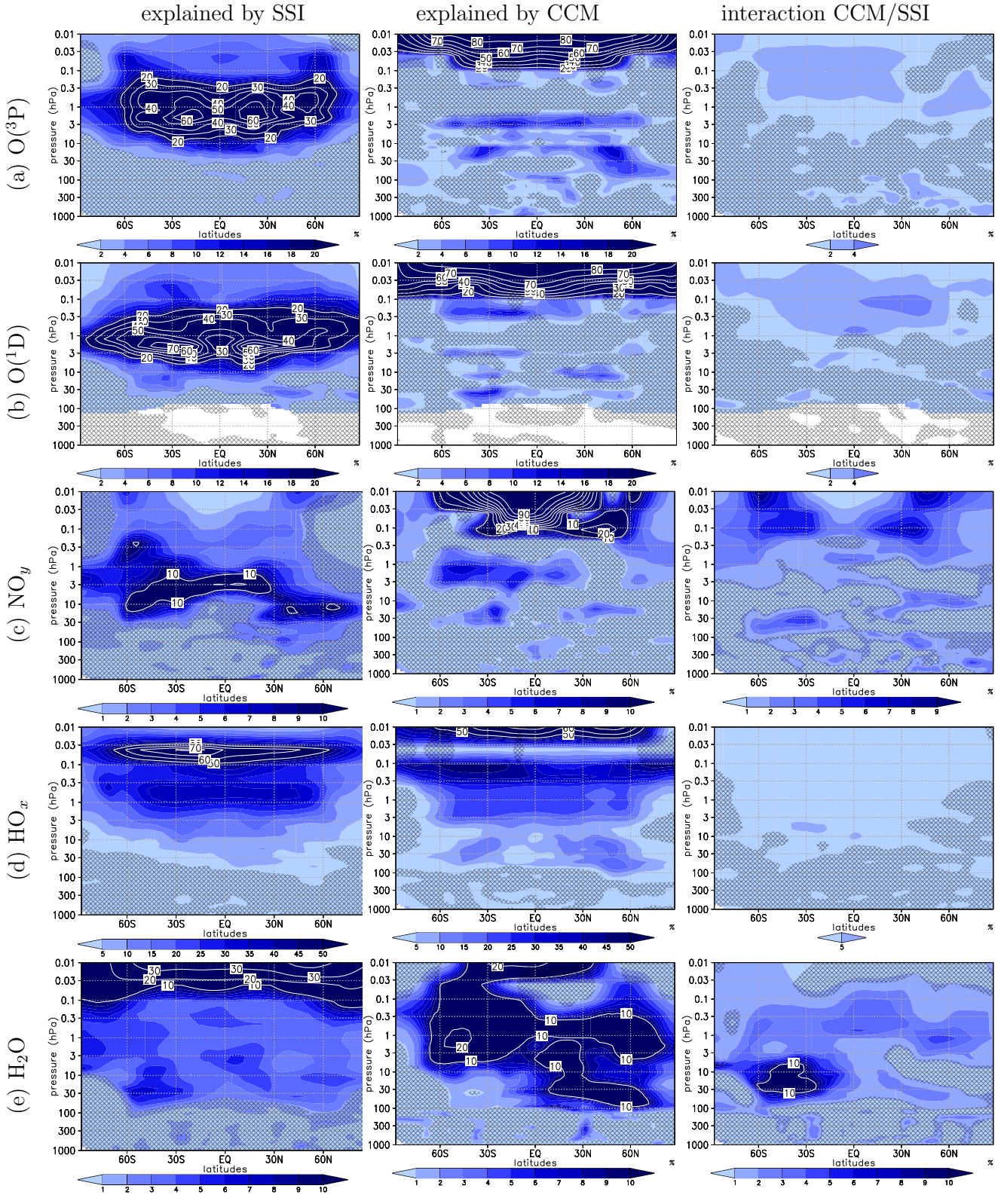

Figure S3: Percentage of solar cycle response variance (square of white contours in Figure 2) explained for (a) $O(^3P)$, (b) $O(^1D)$, (c) NO_y, (d) HO_x, and (e) H_2O mixing ratios. Left column: explained by systematic differences between forcing SSI data sets ($R_{a,B}$ Equation A11, blue shading). The white contours indicate levels of explained variance larger than the range of shading. Middle column: as left column but for systematic differences between CCMs ($R_{a,A}$ Equation A11). Right column: as left column but for signal variance explained by the interaction of the CCM and the SSI data set treatments ($R_{a,AB}$ Equation A12). The grey hatching masks areas where the ratio of explained variance does not pass a test for statistical significance ($p > 5$ %).

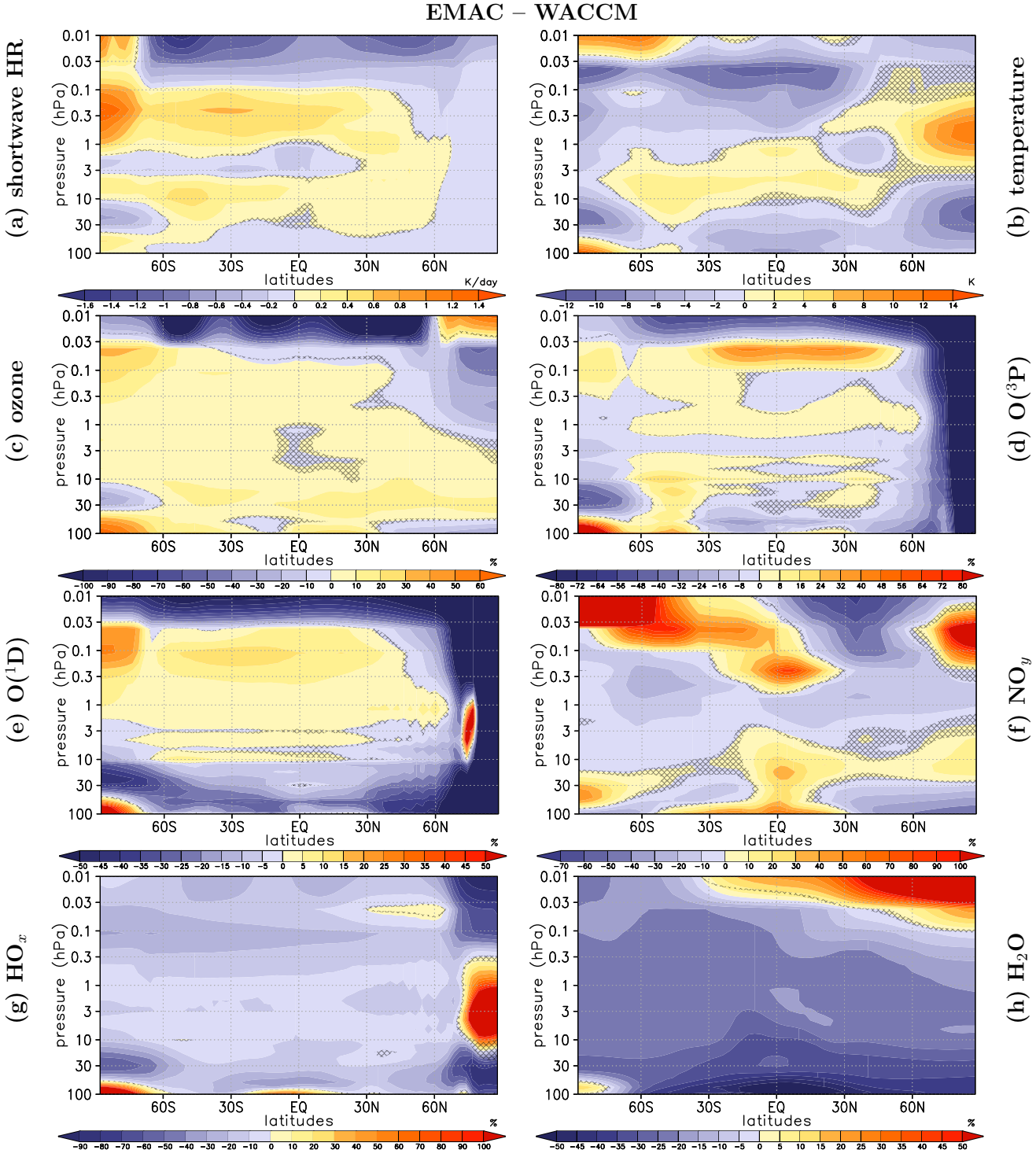

Figure S4: January mean differences for EMAC (ensemble mean) minus WACCM (ensemble mean) (shaded) of (a) shortwave heating rates, (b) temperature, (c) ozone mixing ratios, (d) atomic oxygen ($O(^3P)$), (e) HO_x, and (f) NO_y. The ensemble mean for both CCMs consists of the solar minimum reference simulation (included 5 times in the ensemble mean) and the 5 simulations for the solar maximum. Grey hatching masks areas where differences does not pass a test for statistical significance ($p > 5$ %).

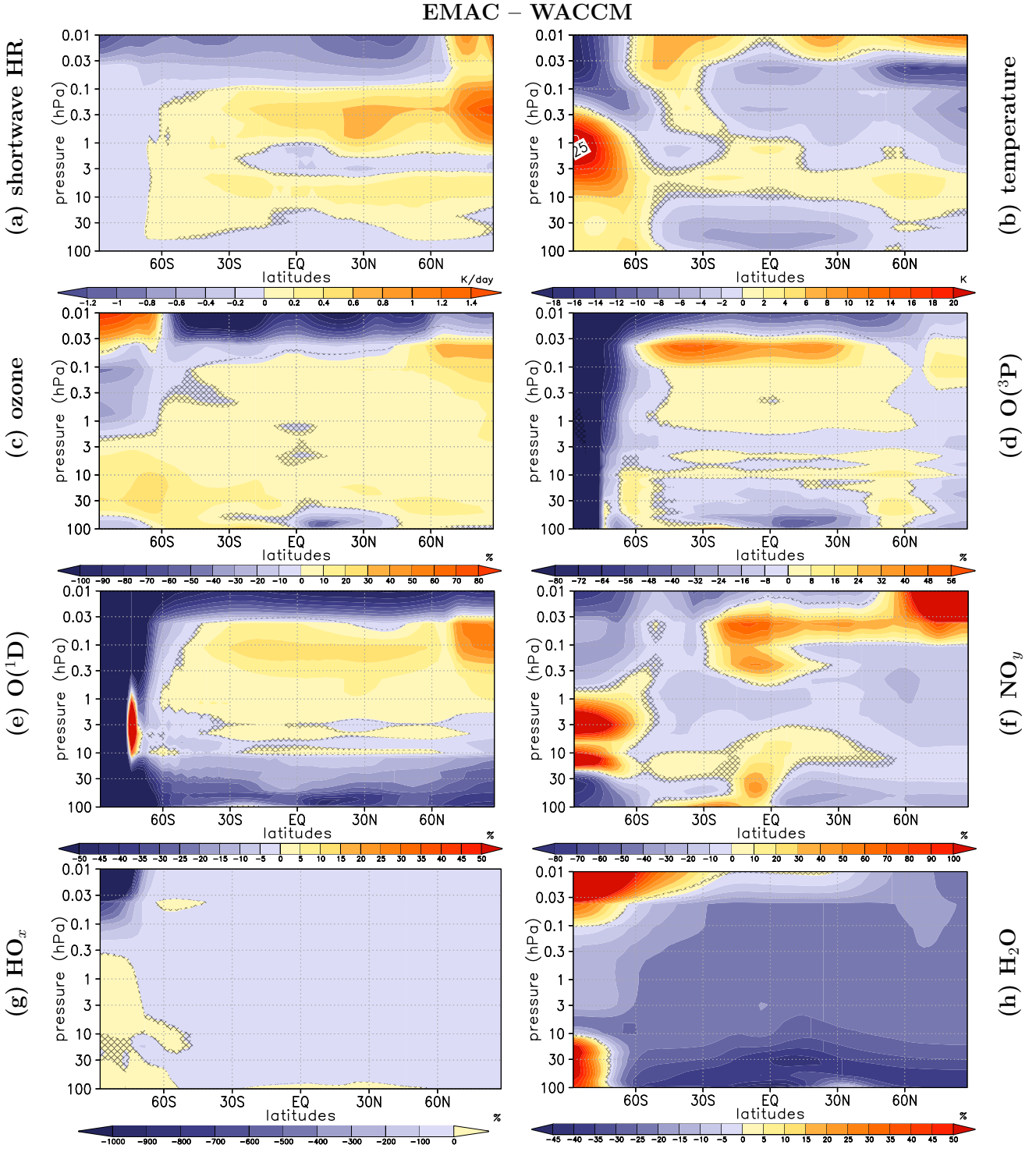

Figure S5: July mean differences for EMAC (ensemble mean) minus WACCM (ensemble mean) (shaded) of (a) shortwave heating rates, (b) temperature, (c) ozone mixing ratios, (d) atomic oxygen ($O(^3P)$), (e) HO_x, and (f) NO_y. The ensemble mean for both CCMs consists of the solar minimum reference simulation (included 5 times in the ensemble mean) and the 5 simulations for the solar maximum. Grey hatching masks areas where differences does not pass a test for statistical significance ($p > 5$ %).

Table S3: Correlation of polar region (70°N–90°N) anomalies (solar maximum – solar minimum) of total column ozone (TCO) and the layer thickness from 100 to 10 hPa. TCO change in DU per 100 m geopotential height change and the 95% confidence interval.

		EMAC		WACCM	
Hemisphere	Season	Correlation	ΔTCO/100 m	Correlation	ΔTCO/100 m
			CMIP6		
NH	Anm	0.82	6.08±0.37	0.68	6.11±0.57
	JFM	0.89	6.79±1.05	0.70	5.49±1.72
SH	Anm	0.81	7.49±0.47	0.77	6.06±0.43
	SON	0.92	8.95±1.14	0.95	5.74±0.61
			SATIRE-T		
NH	Anm	0.81	5.91±0.37	0.69	6.03±0.55
	JFM	0.88	6.14±1.02	0.87	6.29±1.12
SH	Anm	0.82	8.02±0.48	0.76	5.38±0.40
	SON	0.95	9.79±1.02	0.91	5.13±0.73
			SATIRE-S		
NH	Anm	0.83	6.20±0.36	0.71	5.91±0.51
	JFM	0.89	6.75±1.05	0.76	6.31±1.67
SH	Anm	0.81	7.72±0.48	0.69	5.09±0.46
	SON	0.95	9.30±0.89	0.88	4.66±0.78
			NRLSSI1		
NH	Anm	0.84	5.95±0.34	0.70	6.25±0.55
	JFM	0.90	6.00±0.92	0.81	6.96±1.55
SH	Anm	0.82	7.26±0.44	0.76	5.94±0.44
	SON	0.91	8.95±1.24	0.92	5.35±0.70
			NRLSSI2		
NH	Anm	0.82	6.39±0.38	0.66	5.84±0.57
	JFM	0.94	6.48±0.75	0.80	6.81±1.58
SH	Anm	0.83	7.81±0.45	0.76	5.54±0.41
	SON	0.94	9.63±1.10	0.94	5.42±0.61